ARMA 08-126

Back-analysis of elastic properties of the ground using data from a large-scale plate load test

Radončić, N., Grossauer, K. and Schubert, W.
Institute for Rock Mechanics and Tunnelling, Graz, Austria,
Grešovnik, I.
C3M d.o.o., Ljubljana, Slovenia
Gober, H.-J.
KELAG – Kärntner Elektrizitäts-Aktiengesellschaft, Klagenfurt, Austria

This paper was prepared for presentation at San Francisco 2008, the 42nd US Rock Mechanics Symposium and 2nd U.S.-Canada Rock Mechanics Symposium, held in San Francisco, June 29-July 2, 2008.

Using the rock mass as a load bearing element for high pressure hydro-tunnels can lead to considerable reductions in the wall thickness of the steel pipe. For a safe and economical design it is imperative to correctly assess the mechanical properties of the rock mass. The Feldsee project of the Austrian hydro-power company KELAG included an extensive large scale field test program, aiming at the identification of these parameters. The plate load tests were conducted in the tunnel, measuring the force, the absolute displacements of both plates and the displacements in the surrounding rock mass at various depths. Since the results of this kind of test are subject to various influences (problem geometry, loadplate stiffness, mortar bedding), the application of usual closed-form solutions for determining the elastic parameters is questionable. Coupling of a fully three-dimensional numerical model with an optimization routine was used to back-analyze the elastic parameters. The measured data featured asymmetric displacement patterns (and thus: locally differing stiffness) inherent to a heterogeneous rock mass which cannot be properly accounted for in a homogenous numerical model. A simple smoothing and averaging technique was applied to filter out the influences of the heterogeneity and measurement noise. Using the commercial code FLAC3D and its built-in language FISH, the model has been parameterized and coupled with the optimization shell INVERSE. The obtained results are discussed and compared to the currently available semi-empirical equations.

1. INTRODUCTION

The construction of the Feldsee project of the Austrian hydropower company KELAG started in 2006 and is scheduled to be completed by the end of 2008. The basic idea is connecting two existing reservoirs, Feldsee at 2200 m a.s.l. and Wurten at 1700 m a.s.l. in a daily pump storage scheme with a peak power output of 70 MW. Since the startup and shutdown procedures of the turbine have to be rapid (due to the chosen operation scheme and capacity of the reservoirs), the dynamic head reaches 820 m at the lowest part of the pressure tunnel. Motivated by the great cost-saving potential, the design of the pressure tunnel lining treated the surrounding rock mass as an integral and primary load bearing element.

This approach is justified when having the following facts in mind: the rock mass is composed of massive, unweathered gneiss with widely spaced joints of low persistence and the overburden is high enough to allow the development of tensile cracks induced by the internal pressure loading without endangering the global stability of the slope. Assuming the lateral pressure coefficient of 0,4, the calculations have shown that the crack depth under peak internal load does not exceed 10 meters. This is well within boundaries deduced from the hydropower project Häusling, successfully constructed in similar ground conditions. The final solution features pre-cast concrete elements with a thin steel lining in the lowest part of the tunnel and pre-cast concrete elements with a GFRP (Glass Fiber Reinforced Polymer) lining in the upper part (Figure 1).

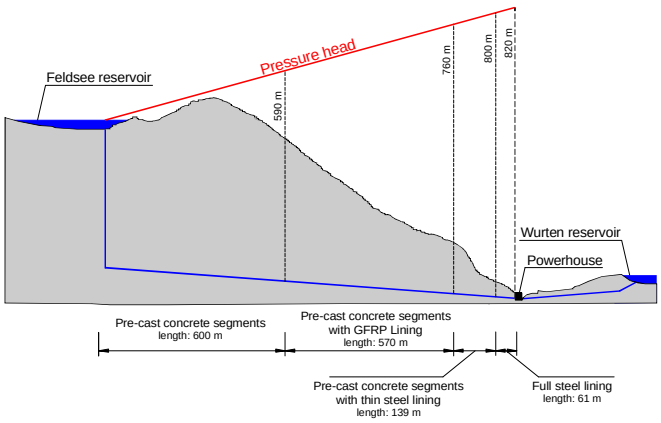

Figure 1: The longitudinal section of the Feldsee project

High pressure grouting under pressure of 40 bar in the gap between the pre-cast segments and the rock mass is planned, effectively pre-stressing it and ensuring its tightness by preventing the generation of cracks. The tightness is granted by the bond with the rock mass after the pre-stressing mortar has hardened, activating the rock mass as an abutment for lining. Since the crack initiation/yield strains of the materials incorporated in the inner lining dictate the maximum radial deformations under a respective internal pressure load, the load displacement behavior of the rock mass and its contribution to the overall system stiffness represent one of the key design parameters. In order to verify the assumptions made in the initial design phase, an extensive field test program has been conducted.

2. TEST CONFIGURATION

The choice of test locations and the test configuration aimed on establishing an envelope of the lowest expectable rock mass properties. Five test cross sections have been selected (Figure 2), each of them identified by the rock mass quality relatively lower then the one encountered in the major part of the tunnel.

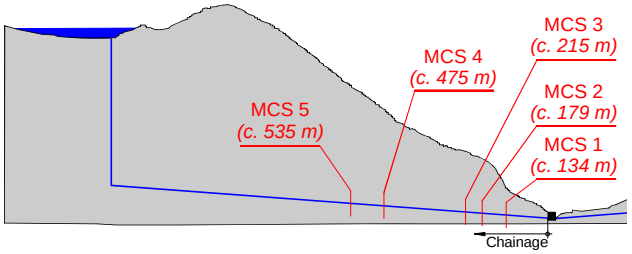

Figure 2: The position of the measurement cross sections

It was decided to perform plate load tests enhanced with an extensive extensometer-based deformation measurement program. In every test location two plate load tests have been performed: one with the loading direction parallel to the foliation orientation and the other one perpendicular to it, addressing the rock mass anisotropy inherent to metamorphic rocks.

The test has been performed with simultaneous loading of both sidewalls, each of them acting as an abutment for the other. The outer diameter of the used load plate was 0.8 m, with a circular opening (0.1 m wide) for the extensometer head in the center of the plate. The hydraulic system allowed loading up to 6000 kN, hence allowing maximum average contact normal stress of 11.93 MPa. One plate has been connected to the piston via ball joint, thus eliminating the influence of eccentric deformation behavior and the occurrence of bending moments in the frame.

In order to ensure tight contact between the load plate and the rock mass, a layer of high strength mortar (measured tangential Young's modulus of 30,000 MPa) has been cast between the contact steel plate (thickness of 10 mm) and the rock mass (Figure 3). The thickness of the mortar layer varied according to the roughness of the sidewall, but never exceeded 30 cm.

The displacement monitoring was performed by utilizing a single magnetic extensometer aligned with the axis of the load plate. It measured the displacement of four magnets which were stiffly bonded with the rock mass. On every side, they were positioned at the depths of approx. 30, 50, 125 and 230 cm measured from the outward rim of the load plate (Figure 3).

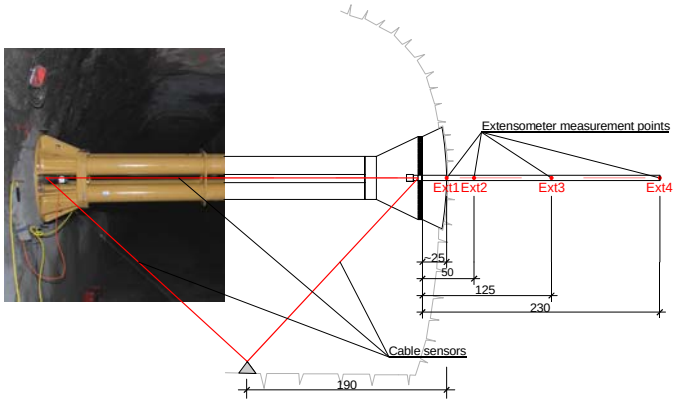

Figure 3: The test geometry and sensor set-up (in cm)

The displacement of the load plates has been monitored by three cable displacement sensors. With the assumption that the third, external fixing point does not move during the test (which is justified, when we take into account the magnitude of the observed load plate and extensometer displacements), the absolute displacements of both load plates are easily calculable.

3. IMPLEMENTATION BACKGROUND

The numerical parameter estimation from data which do not allow direct measurement of physical parameters is being used for years in the field of mechanical engineering and related disciplines. The reason for its slow development in the field of rock mechanics lies in the character of the accessible data: the input information for a numerical back analysis should allow unambiguous identification of the model parameters. Simply put, the true values of the stress field in the rock mass are usually not known and have to be assumed. Hence, a back analysis performed solely on the basis of the measured deformations leads to a mathematical problem without a singular solution - there is an infinite number of mechanical parameters leading to the same displacement field (if the "other side of the equation", the kinetic quantities, are unknown). Another obstacle is being presented by the highly complex mechanical behavior of the rocks: the state-of-the-art constitutive laws represent mere approximations of differing quality – none of them generally applicable to all situations.

The plate load test however, especially in this particular case, *does yield* enough information for a back-analysis, since both the displacements and the respective force are determined. The test set-up has been regarded as very favorable due to the existence of displacement measurements *in the rock mass*, minimizing the possible ambiguities in the solution. Another favorable aspect was the high quality of the rock mass itself: the stress level in the secondary stress state has been deemed well below the rock mass strength (thus minimizing the non linear aspects of the deformation behavior of the ground).

3.1. Technical implementation

The inverse identification of model parameters based on a numerical model and measurements can be simply defined: we seek for parameters **x** of the model such that the model response corresponds as much as possible to the measurements obtained in the test. The identification problem is thus defined as:

$$\begin{aligned} &\text{minimize} && f(x), x \in R \\ &\text{subject to} && c_i(x) \le 0, i \in I \\ &\text{and} && l_k \le x_k \le u_k, k = 1,2,...n\,. \end{aligned}$$

In the above formulation, $f(x)$ is the objective function that measures the discrepancy between actual measurements and the corresponding quantities calculated by the numerical model. The functions $c_i(x)$ are constraint functions that ensure physical consistency of parameters (for instance: positive real value for Young's modulus). The values l_k and u_k define the meaningful *a priori* bounds for the sought after parameters. The requirements for the technical implementation of such a procedure are straightforward.

- bilateral communication between the numerical model and the optimization routine minimizing the objective function;
- automatic assignment of the input parameters in the numerical model and
- reading of the target model values and the calculation of the objective function value

have to be granted. In our case, all of these requirements have been met by using the built-in scripting language of the FLAC3D commercial solver.

The communication has been ensured by defining input and output file formats being generated and interpreted by FLAC3D and the optimization shell INVERSE. The set of target values has been also provided in the form of an external file, being loaded into memory at the beginning of every new analysis (Figure 4).

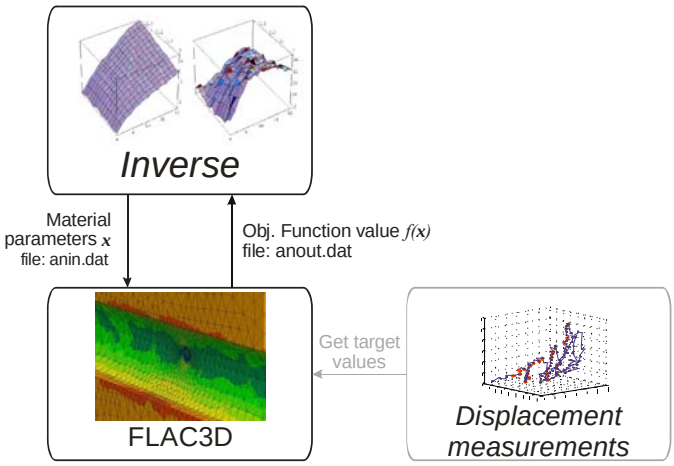

Figure 4: the implemented architecture and relationships between INVERSE, FLAC3D model and target values

In order to ensure numerical stability of the model, the model geometry was generated prior to the start of the back-calculation procedure and has been restored in every new run.

3.2. Numerical model

The model geometry and the associated mesh have been generated in the commercial FE and modeling package ABAQUS and then transferred into FLAC3D. Although the accuracy drawbacks associated with tetrahedron meshes are generally well-known and documented [1], it was still decided to use these elements, since they allow meshing of almost arbitrary geometries and with very high element size gradients. Simply put, because the calculation speed is such a crucial factor when performing parameter identification as proposed here, the used mesh has to be highly efficient and only relevant parts of the model have to feature high calculation accuracy.

Before the back analysis of the ground properties was started, rigorous testing of the model behavior has been performed:

- Since the stiffness of the load plate has high influence on the stress field in its vicinity, the contact plate, the mortar and the rock mass have been modeled in an axisymmetric FE model. The check of both extreme cases of infinitely stiff (rigid) plate with prescribed uniform displacements of the contact area and infinitely soft plate with uniform normal stress loading lead to the conclusion that the influence of the load plate stiffness is negligible on the displacement field behind the mortar layer (in the expected range of mechanical parameters of the rock mass). Therefore the loading has been applied as uniform loading at the contact boundary between load plate – mortar while omitting the plate geometry, thus considerably reducing the number of elements in the model;

- The displacement field calculated by the used model (with the "mortar region" having the same material properties assigned as the surrounding rock mass) has been checked against the displacement field obtained from the closed-form solution [2]. The results are plausible – the far field results should be ignored due to truncation effects of the boundary conditions (Figure 5).

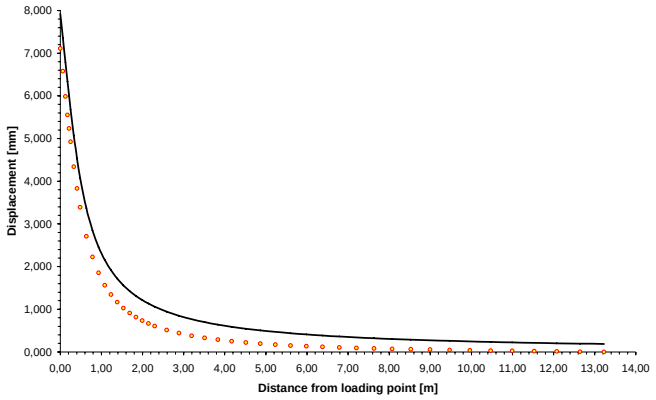

Figure 5: comparison between the displacements obtained from the Boussinesq solution (black) and the displacement field from the used numerical model (dots).

The initial work with the numerical model used the double yield constitutive law provided with FLAC3D. It has the ability to model arbitrary volumetric plastic increments and utilize two different load-displacement relationships for the branches of first loading and un-/re-loading. However, its usage proved to slow down the calculations considerably and result in rather sluggish response to the changes of the model parameters – the reason lying probably in its combination with tetrahedral elements.

Consequently, the calculations have been performed using elastic parameters, with the model switching "manually" between the respective first loading and re-/un-loading parameters. Although this might not be regarded as the most elegant solution to the problem, it proved to be numerically stable, fast and yielded very plausible material parameters.

3.3. Treatment of the test data

The test results imply a considerable amount of heterogeneity, with (sometimes) very different displacements measured at the respective sides of the tunnel. Additional problems were posed by the high amount of logged data (calculating all logged loading steps would have lead to an extreme increase of calculations times without a significant improvement of the results) and the fact that certain amount of time had to pass before the rock mass reached its new equilibrium under every loading step (Figure 6a).

In order to counter these circumstances, we decided to attempt the inverse analysis of test results obtained from the horizontal test ran at the tunnel chainage 179. They exerted almost a symmetrical response in all measurements, so we averaged the test results from the left and right side, thus allowing the calculation of a half-model with symmetrical boundary conditions. The filtering of the measurement data and the identification of relevant points in the load-displacement plot was solved in a straightforward way. The calculation of the first derivative (approximated by the backward finite difference) of the load-time curve allowed very reliable determination of the relevant test points, considerably reducing the amount of data. In the next step, the final target values have been chosen manually, using engineering judgment.

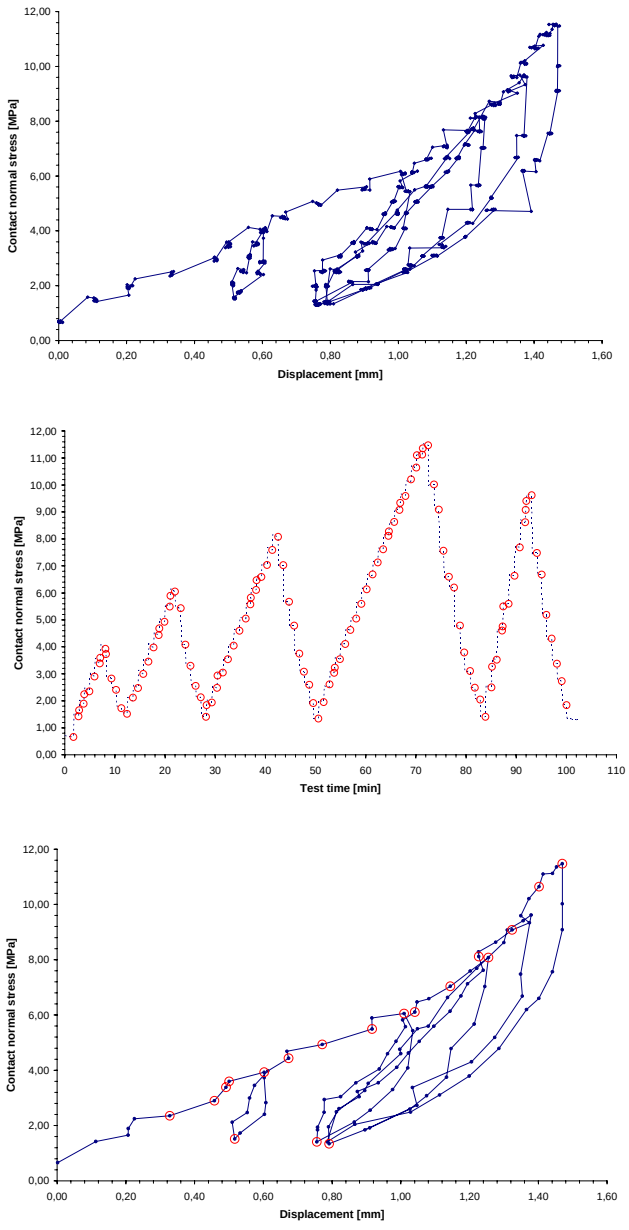

Figure 6: the applied filtering procedure. With the calculation of the derivative of the loading with respect to time (b) the raw data (a) can be filtered towards the more transparent set (c). The red circles in (c) mark the target values.

The un-/re-loading loops have been taken into account by the selection of their starting point, their turning point (lowest load reached) and their ending point (where the applied load dictated a switch to the first-loading branch).

3.4. Definition of the objective function

The objective function was implemented as a weighted square of normalized errors. This somewhat cryptic verbal definition is actually very simple to explain: due to the fact that the magnitude of the displacement readings decreases with the increasing extensometer depth, the influence of the deep readings would be completely lost in the overall sum of squared errors. Hence, some kind of normalization of the results had to be implemented, giving every reading the same weight and importance. On the other hand, the readings from the extensometers 3 and 4 feature a great amount of noise (Figure 7), sometimes even featuring negative tangential moduli in the loading-unloading loops. The contribution of the deep extensometers to the overall evaluation of the fit between the numerical model and measurements should therefore be decreaseable in a controlled fashion.

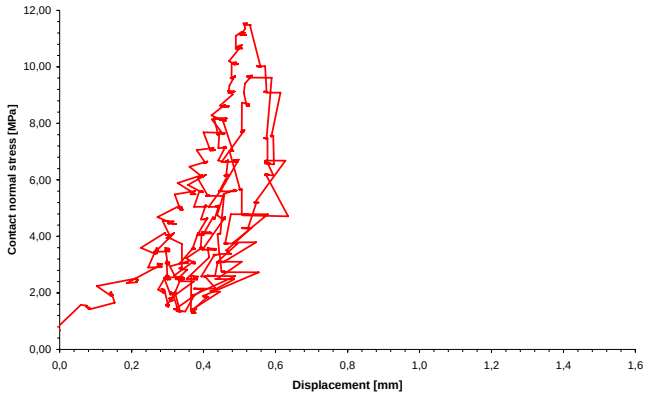

Figure 7: Load-displacement path of the extensometer 4 (distance from the load plate: 230 cm)

Incorporating the above requirements, the objective function can be written as:

$$f(x) = \sum_{j=1}^{k} \sum_{i=1}^{l} \left(w_i \cdot \frac{u^*_{ji} - u_{ji}}{\tilde{u}_{ji}} \right)^2 \qquad 1$$

wherein x is the vector of model parameters, u^*_{ji} are the target values measured by the sensor i for the loading step j, u_{ji} represents the associated values obtained from the numerical model and w_i are the weights assigned to the readings of the sensor i.

3.5. Model parameterization

The vector of material parameters has been kept rather small in all cases: during the testing phase and synthetic runs with "dummy" data, the input for the double yield constitutive law was defined as $\boldsymbol{x}=\{K, K_c\}$, wherein K and K_c represent the elastic and plastic bulk modulus (defining the relationship between volumetric plastic strain and hydrostatic stress component), respectively. If the Poisson's ratio ν is known, all other model parameters can be derived from these two values (assuming, as already stated, that no deviatoric yielding takes place in the model).

After the switch to linear elastic material behavior as documented in 3.3, the model parameters vector was defined as $\boldsymbol{x}=\{E, R\}$, wherein E represents the un-/re-loading Young's modulus and R represents the ratio between the moduli of the un-/re-loading and first loading loops. This formulation ensures model consistency in all cases, eliminating the need for constraining the first loading modulus to be lower then or equal to the modulus of the un-/re-loading loop.

3.6. The applied optimization algorithm

The optimization problem is usually most efficiently solved by Quasi-Newton or conjugate gradient methods in the cases where constraints are not present [3,4,5] or by sequential quadratic programming methods in case of constrained problems [3,6]. In order to apply these methods, gradients of the objective and constraint functions must be provided.

In our case the main obstacle with providing gradients was that the analytical derivatives with respect to model parameters could not be obtained from the FLAC3D model, hence leaving the numerical differentiation as the only alternative. It is widely agreed that application of the above mentioned methods in combination with finite difference approximation of gradients still provides the most efficient approach for the solution of a wide range of problems with twice differentiable response functions. Many practical examples confirm this, but with a significant caveat that must be considered in all cases where complex numerical models are used for calculation of the response functions, namely that the effect of numerical noise in response functions must be carefully observed [7]. Since numerical differentiation is sensitive on noise, automatic application of optimization techniques using numerical gradients is prone to erroneous results or complete breakdown of the solution procedure.

In the presented example, the level of numerical noise contained in the response functions was first studied on a synthetic case, in which the same numerical model was used as in the real case, but with measurements artificially generated by the numerical model with the assumed values of the searched material parameters. Use of such synthetic cases is applicable for verification and performance studies of solution procedures because the precise solution is known in advance.

Figure 8 shows the objective function tabulated on a line between two points in the parameter space, where

synthetic measurements generated by the same model are used in the definition of the objective function. The same numerical model was used as for true parameter identification. The objective function is tabulated between the assumed "true parameters" $\boldsymbol{x}^*=\{500,2000\}$ and between $\boldsymbol{x}=\{15000, 5000\}$. Geometrically growing sampling intervals with elongation factor 1.4 were used, which enables zooming of very small intervals close to the first point with reasonable number of calculated points. The objective function seems to be smoothly differentiable when plotting the whole sampled interval (Figure 8a). Numerical noise is observable when a small and densely sampled interval is zoomed in (Figure 8b).

The results indicated that the level of noise contained in the response is too high to safely apply numerical differentiation of the response without taking costly measures to increase precision of numerical computations. This being said, it has to be stated that the amount of noise when using FLAC3D can be reduced to a certain degree with the applied criterion of model equilibrium. We used the maximum gridpoint velocity of 10^{-7} "m/s" as the criterion, the calculation stopping the solving procedure after all gridpoint velocities have fallen below this limit. In parameter studies this threshold proved to be a good compromise between computation speed (one model run taking between 5 and 10 minutes) and result precision. The bottom line is that it is impossible to remove the noise completely from model response; due to the discretization and numerical roundoff errors it is inherent to every numerical method.

After considering the above circumstances we decided to use an optimization method that does not make direct use of gradient information or perform noise sensitive numerical operations.

The Nelder-Mead simplex method [5,8] was identified as a method of choice as it provides a reasonable compromise between the efficiency and robustness. This method maintains a simplex defined by n+1 points in the design space in which the objective function is evaluated. Throughout iterations, it accommodates the simplex by merely comparing function values in its apices. The simplex searches the design space according to a set of possible steps designed to prevent degeneration and ensure progress towards minimum (Figure 9). Which step is taken in each iteration is decided by successive attempts of moving particular simplex apices followed by evaluation of new function values and comparison with the old ones.

The Apex with the highest function value (or "the worst point") is first reflected over the center of other apices (step a in Figure 9). If the function value in the reflected point is smaller than original one then expansion is attempted (step b). Otherwise, the algorithm tries to move the worst point towards the point of reflection, which causes contraction of the simplex (steps c and d). If this also doesen't yield a better point then all other apices are moved towards the best pont (step e).

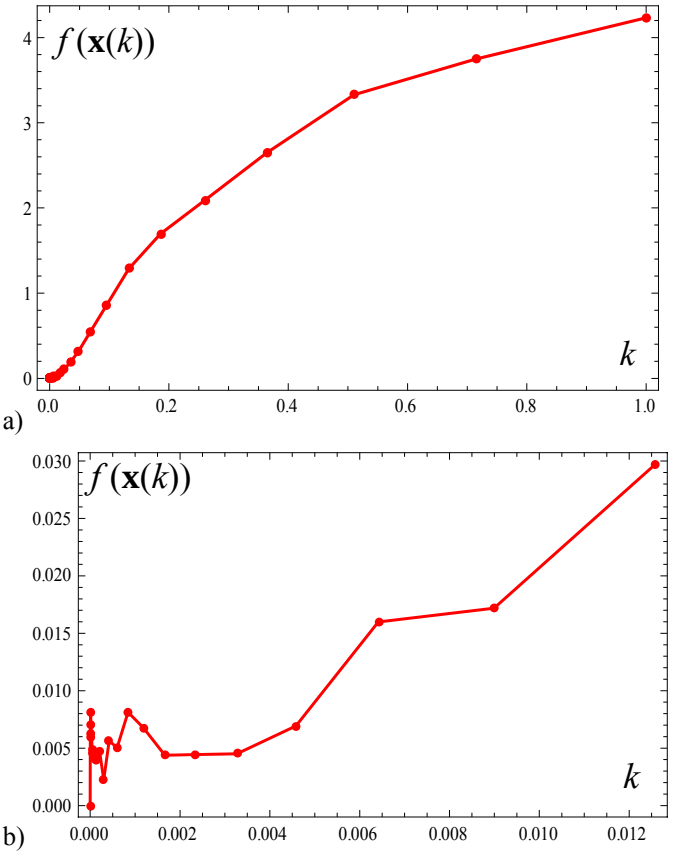

Figure 8: Tabulated objective function between two points in the parameter space utilizing a synthetic model. Figure a) shows the full interval and b) zooms the part close to the origin. Linear factor running from 0 in the first point to 1 in the second point of the line is shown in the horizontal axis, and the objective function value on the vertical axis.

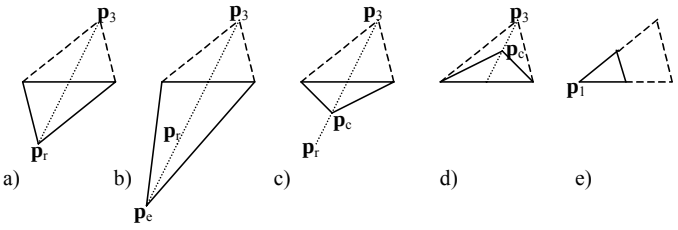

Figure 9: Possible steps of the simplex algorithm in two dimensions with characteristic points: a) reflection, b) expansion, c) outside and d) inside contraction, and e) shrink.

Relative robustness of the method can be assigned to the fact that very little information about the minimized function is directly analyzed and exploited, while the method is still capable of reasonable response to features such as change in the gradient direction or ratio between gradient size and mean curvature. The order of local convergence is linear, but the rate may become slow if problem parameters are not well scaled [8].

In the presented example, the NLPSimp (nonlinear programming simplex) method [9] was used, which is a modification of the Nelder-Mead method adapted for solving constrained optimization problems. One of the modifications is related to the definition of a new comparison operator, which compares the calculated response first by values of violated constraint functions (if any) and then by the value of the objective function. Bound constraints are treated in a specific way such that the numerical simulation is never performed at the parameters that are out of the prescribed way. This is achieved by a combination of parameter transformation that project out-of-bounds parameters to the correspoinding bounds, and addition of a penalty term to the objective function in order to discriminate between parameters in infeasible region according to the amount of constraint violation. Such treatment of bound constraints is beneficial in the cases where infeasible parameters would cause breakdown of the numerical model (e.g. a negative Young's modulus or the Poisson's ratio greater than 0.5).

4. RESULTS

The back analysis of the ground properties from the horizontal test at the chainage 179 was performed in three steps.

First, the elastic parameters E and v have been identified based only on the loading branch of the test. This has lead to the estimation of the Poisson's ratio v. Assuming that it stays constant both throughout the first loading and un-/re-loading branch ([1], 10), this parameter was fixed in the further back-analysis runs, hence reducing the number of sought after model parameters. The procedure yielded plausible parameters (Table 1).

Table 1: Results obtained from the first back-analysis run and the evolution of the associated objective function

Young's modulus E (first loading branch)	[MPa]	3,387.03
Poisson Ratio v	[-]	0.10
Start value of the objective function:	[-]	4.594
Final value of the objective function:	[-]	0.739

The experience from this first back analysis run showed that the convergence of the optimization algorithm slightly increases if the weights of the extensometer 3 and 4 measurements are set to 0.25, while no adverse effects on the final result can be observed. The load plate displacement appeared to be physically inconsistent with the rest of the measurements, with a certain amount of contact stiffness not accountable for in the model. Hence, the weight of the load plate displacement was set to zero, and the extensometer 1 and 2 displacement measurements have been assigned the weight of 1.0.

4.1. Complete loading-unloading analysis

In the next step, the entire set of target values was used, featuring multiple switches between first loading and un-/re-loading loops. The parameters obtained show plausible agreement with the parameters obtained from closed-form solutions [2,10].

Table 2: Results of back analysis for the entire set of target values

Young's Modulus E (un-/re-loading branch)	[MPa]	8,949.36
Ratio between E and V	[-]	2.53
Deformation Modulus V (first loading branch)	[MPa]	3537.29
Start value of the objective function	[-]	32.90
Final value of the objective function	[-]	0.679

4.2. Complete analysis incorporating high performance mortar bedding

After both back-analysis runs proved to be convergent and stable, the back analysis of rock mass properties incorporating the influence of the high performance mortar was started. The results, if compared to the ones in Table 2, show a plausible decrease of the rock mass properties, since the stiff mortar bedding acts as a load distributing element, reducing the concentration of stresses below the load plate (Table 3).

Table 3: rock mass parameters with the influence of bedding mortar incorporated

Young's Modulus E (un-/re-loading branch)	[MPa]	7,716.31
Ratio between E and V	[-]	2.49
Deformation Modulus V (first loading branch)	[MPa]	3,098.93
Start value of the objective function	[-]	18.34
Final value of the objective function	[-]	0.700

After inspecting the plots of calculated and measured load-displacement relationships for every sensor position, a very good fit between Extensometer 1 and associated model response was observed, however the deeper extensometers featured stiffer behavior than anticipated. The reason lies in the zone around the cavity damaged by blasting, inducing micro-cracks and thus considerably reducing the stiffness of the rock mass. Attempting the identification of the mechanical properties of the unaffected zone, the weight assigned to Extensometer 1 was reduced to 0.25, effectively

allowing the algorithm to freely fit the measurements obtained from the deeper positions. The results are presented in Table 4.

Table 4: Rock mass parameters obtained from deeper extensometers

Young's Modulus *E* (un-/re-loading branch)	[MPa]	9525.94
Ratio between *E* and *V*	[-]	2.78
Deformation Modulus *V* (first loading branch)	[MPa]	3426.59
Start value of the objective function	[-]	21.46
Final value of the objective function	[-]	0.649

As expected, the results show an increase of the rock mass parameter values (when compared to the results presented in table 3), confirming the existence of a damage zone. Unfortunately, a rigorous identification of the damage zone extent would also dictate geometrical parameterization, which is currently technically impossible. The considerable amount of noise in the readings of Extensometers 3 and 4 represents one further obstacle, rendering the combination of geometrical case studies (variation of the damage zone extent already incorporated while generating the model mesh) and back analysis for parameter determination unfeasible.

4.3. Discussion

The obtained results have been checked on their plausibility by comparing them to the state-of-the-art closed-form solutions [2, 10]. The results are presented in Figure 10.

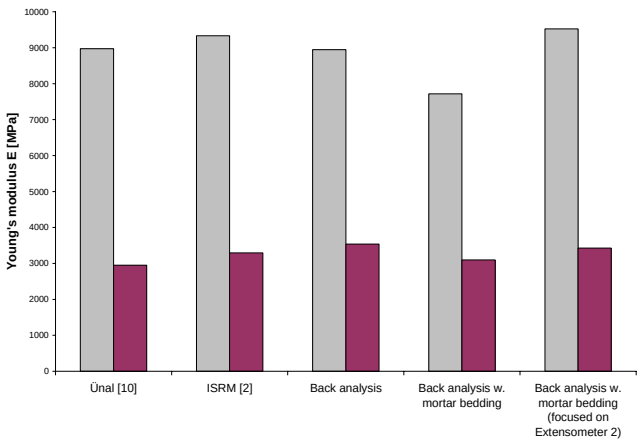

Figure 10: Rock mass parameters obtained by different relationships (grey: un-/re-loading modulus, red: first loading modulus)

The presented comparison backs the correctness of the results. Although the boundary influence in the numerical model poses a drawback that has to be accepted when performing this kind of back-analysis, the ability to incorporate additional influences of geometrical and mechanical deviations from the idealized closed-form solutions represents (in certain cases) a valuable addition. The relative error (with respect to the results of back-analysis with the mortar layer) of the Ünal and ISRM results shows that the bedding has a considerable influence on the outcome of the analysis (Table 5).

Table 5 Overview of the relative error with respect to the back-analysis results

	V [%]	*E* [%]
Ünal solution	16.3	4.7
ISRM recommendation	21.0	6.3

5. CONCLUSION

The motivation for this work has been somewhat broad: apart from wanting to determine the rock mass properties with as low amount of simplification as possible, we also wanted to test the developed optimization algorithm and its behavior when coupled with FLAC3D. The conclusions, when applied to the field of rock mechanics, lie at hand:

- The back analysis is applicable only when an unambiguous set of measurement data is available. Hence, if trying to identify the material parameters, some information about the stress field must be available as well.
- The state-of-the-art optimization algorithms developed and implemented by C3M are efficient, stable and can be used with the commercial Itasca Code FLAC3D.
- The used constitutive law must be able to depict the true material behavior at a satisfactory level; otherwise the obtained fit is meaningless.
- If the requirements stated above are met, the inverse identification of material parameters using numerical models can be deemed as probable to succeed, disregarding the issue of enormous calculation times in some cases.

The future work will concentrate on solving problems with the stability of the double-yield model, since it would allow the incorporation of arbitrary (also non-linear) volumetric hardening relationships. This would allow meaningful parameter identification also in cases of measurements featuring non-linear load-displacement relationships. Another aim is the combination of the double yield model with elastic orthotropy. In ideal case, the back analysis would consider the measurements obtained from both vertical and horizontal tests and end in identifying the rock mass properties which are

invariant to the test orientation. On the long term, the back analysis of rock mass properties based on absolute displacement monitoring in tunnel construction is envisioned.

The authors would like to express their gratitude to the KELAG Kärntner Elektrizitäts-Aktiengesellschaft for granting access to their test results.

This work was partially funded by the research project TunConstruct, part of the 6th frame program of the European Union.

REFERENCES

1 Itasca Consulting Group, Inc. 2005. *FLAC 3D User's manual*. 2nd Edition. Minnesota

2 International society for rock mechanics. 1978. Suggested methods for determining in situ deformability of rock. In. *Rock characterization testing and monitoring*., ed. E.T.Brown, 143-148

3 Fletcher, R. 1996. *Practical methods of optimisation.* 2nd edition. NewYork: John Wiley and Sones.

4 Press, W.H., Teukolsky, V.T., Vetterling, V.T., Flannery, B.P. 1992. *Numerical recipes in C – the art of scientific computing*. 1st edition. Cambridge: Cambridge University Press.

5 Grešovnik, I. 1995. *A general purpose computational shell for solving inverse and optimisation problems – applications to metarl forming processes*, PhD Thesis, available at http://www.c3m.si/inverse/doc/phd/index.html

6 Zhou, J.L. and Tits, A.L. 1996. An SQP Algorithm for finely discretized continuous minimax problems and other minimax problems with many objective functions. *SIAM Journal on optimization 6/2:* 461-487

7 Ibrahimbegović, A., Grešovnik, I., Markovič, D., Melnyk, S. and Rodič, T. 2005. Shape optimization of two-phase material with microstructure. *Engineering computations* 22/5, 605-645

8 Wright, M.H. 1996. Direct search methods: once scorned, now respectable. *In Proceedings of the 1995 Dundee biennial conference in numerical analysis,* eds. D.F. Griffiths et al, 191 – 208. Harlow: Addison Wesley Longman.

9 Grešovnik, I. 2007. *Solving optimization problems by the optimization program inverse.* Electronic document at: http://www.c3m.si/inverse/doc... /main/latest/invopt.pdf

10 Ünal, E. 1997. Determination of in situ deformation modulus: new approaches for plate-loading tests*. International journal of rock mechanics and mining sciences* 34: 897 - 915